Prefrontal spatial working memory network predicts animal's decision-making in a free choice saccade task.

Kei Mochizuki[1] and Shintaro Funahashi[1,2]

1. Kokoro Research Center,
Kyoto University, Kyoto, Japan.
2. Laboratory of Cognitive Brain Science,
Department of Cognitive and Behavioral Sciences,
Graduate School of Human and Environmental Studies,
Kyoto University, Kyoto, Japan.

Running Head: Decision-making in a free choice saccade task

Address for Correspondence:

Shintaro Funahashi
Kokoro Research Center, Kyoto University
46 Yoshida-Shimoadachi-cho, Sakyo-ku, Kyoto 606-8501, Japan
funahashi.shintaro.2z@kyoto-u.ac.jp

Abstract

While neurons in the lateral prefrontal cortex (PFC) encode spatial information during the performance of working memory tasks, they are also known to participate in subjective behavior such as spatial attention and action selection. In the present study, we analyzed the activity of primate PFC neurons during the performance of a free choice memory-guided saccade task in which the monkeys needed to choose a saccade direction by themselves. In trials when the receptive field location was subsequently chosen by the animal, PFC neurons with spatially selective visual response started to show greater activation before cue onset. This result suggests that the fluctuation of firing before cue presentation prematurely biased the representation of a certain spatial location, and eventually encouraged the subsequent choice of that location. In addition, modulation of the activity by the animal's choice was observed only in neurons with high sustainability of activation, and was also dependent on the spatial configuration of the visual cues. These findings were consistent with known characteristics of PFC neurons in information maintenance in spatial working memory function. These results suggest that pre-cue fluctuation of spatial representation was shared and enhanced through the working memory network in the PFC, and could finally influence the animal's free choice of saccade direction. The present study revealed that the PFC plays an important role in decision-making in a free choice condition, and that the dynamics of decision-making is constrained by the network architecture embedded in this cortical area.

Keywords:

Prefrontal cortex, Spatial representation, Decision-making, Memory-guided saccade

Introduction

Neurophysiological investigations of the prefrontal cortex (PFC) have shown that neurons in the lateral PFC exhibit a persistent activation during the delay period (delay-period activity) when the monkey is remembering a particular spatial location in memory-guided saccade tasks (Funahashi et al. 1989, 1990, 1991, 1993b; Goldman-Rakic et al. 1990; Constantinidis et al. 2001a, 2001b). This delay-period activity has been proposed to be a neuronal correlate of active maintenance of visuospatial information. The role of the PFC in information maintenance has been further supported by lesion studies in monkeys (Funahashi et al. 1993a; Sawaguchi and Iba 2001) and humans (D'Esposito and Postle 1999; Mottaghy et al. 2002; Müller et al. 2002), and by functional brain imaging studies (Courtney et al. 1998; Zarahn et al. 1999, 2000; Sakai et al. 2002). Thus, the maintenance of task-relevant spatial information could be one of the key features that could help us to understand the function of the PFC (Fuster 2008).

Spatially selective activity of PFC neurons has also been proposed to be related to decision-making process such as response selection (Rowe et al. 2000) and spatial attention (Lebedev et al. 2004; Messinger et al. 2009). Especially, in human neuroimaging studies, the PFC has been reported to play a role in self-initiated behavior and internally-driven decision-making (Frith et al. 1991; Hyder et al. 1997; Lau et al. 2004a, 2004b; Haynes et al. 2007; Soon et al. 2008). Therefore, the known

61 characteristic activation of spatially selective PFC neurons could also be related to
62 decision-making under these situations. Previous studies have investigated the
63 neuronal underpinning of decision-making under these situations in the PFC
64 (Watanabe et al. 2006; Watanabe and Funahashi 2007) and other related areas such as
65 frontal eye field, supplemental eye field and lateral intraparietal cortex (Coe et al.
66 2002). These studies reported that the activity of spatially selective neurons is related
67 to the animal's own decision about saccade direction. However, in these studies, a
68 fixed set of spatial locations were repeatedly presented as options for a saccade in a
69 block of trials. Under this setup, presentation of the spatial cues was less informative
70 since the available saccade directions were obvious without seeing the actual cue
71 presentation. The monkey could indeed decide the saccade direction before the
72 presentation of the visual cues. In addition, due to the predetermined and less various
73 configuration of the cues, precise analysis about the relationship between neuron's
74 receptive field and chosen location was limited. Therefore, further experiment which
75 enables a close examination of how prefrontal working memory network represents
76 multiple spatial information and how the activity of PFC neurons is related to the
77 animal's own decision about saccade direction is needed.
78 In the present study, we established a free choice memory-guided saccade task in
79 which the monkeys by themselves chose the direction of the saccade among multiple
80 locations changing trial to trial. By varying the options for a choice in each trial, we
81 could examine the precise time course of decision-making process taken in the

network of spatially selective PFC neurons. We found that the activity of lateral PFC neurons could predict the animal's decision about subsequent eye movement direction even before cue presentation. This suggests that pre-existing activation state of PFC neurons immediately before cue presentation influenced the construction of spatial representation, and eventually biased the animal's subsequent choice of the saccade direction. Furthermore, we found that the impact of neuron's activity on the animal's choice was stronger in neurons that showed greater persistent activity in a control spatial working memory task. In addition, while PFC neurons tended to represent unchosen spatial location more weakly from the beginning of the trial, this suppression of unchosen location was modest when chosen and unchosen locations were placed in the same side of the visual field. This finding was in accord with the known contralateral organization of spatial working memory network in the PFC. These results indicate that the role of PFC neurons in a free choice of saccade direction is linked to their firing property and network background as a neuronal underpinning of spatial working memory function. Our present study showed a possible overlap of cellular mechanisms for maintenance and decision-making of spatial information, and offers a clue to a further investigation on the nature of the spatial information processing taken place in the PFC.

Materials and Methods

Animals

We used two female Japanese monkeys (*Macaca fuscata*; monkeys O and E). The monkeys were housed in individual stainless steel home cages. Water intake was restricted in the home cage and provided as a reward in the laboratory. Additional vegetables and fruits were provided to fulfill the daily requirement of water intake if necessary. All experimental procedures were conducted in accordance with the guidelines provided by the Primate Research Institute of Kyoto University and were approved by the Animal Research Committee at the Graduate School of Human and Environmental Studies, Kyoto University.

Apparatus

During experimental sessions, the monkey sat in a primate chair in a dark sound-attenuated room with its head movements restricted by a head-holding apparatus. We used TEMPO software (Reflective Computing, Olympia, WA, USA) for task control and data acquisition. Visual stimuli were presented on a 20-inch CRT monitor (Dell UltraScan D2026T-HS, Dell, Round Rock, TX, USA) that was placed 40 cm from the subject's face. A scleral search coil system (Enzanshi Kogyo, Tokyo, Japan) was used to monitor the monkeys' eye movements (Robinson 1963; Judge et al. 1980).

Tasks

We used two types of memory-guided saccade tasks (Fig. 1a): an Instructed Choice Task (ICT) and a Free Choice Task (FCT). The tasks were similar to those used in previous studies (Watanabe et al. 2006; Watanabe and Funahashi 2007; Mochizuki and Funahashi 2014). In both tasks, a trial started with the presentation of a fixation point (white cross, 0.5° in visual angle) at the center of the monitor. After the monkey maintained fixation on the fixation point for 1.0 s (fixation period), eight peripheral targets (white cross, 0.75°) were presented at an eccentricity of 13° (0°–315°, separated by 45°). The monkey had to neglect these targets and keep watching the fixation point for another 1.0 s (pre-cue period). Next, one or two visual cues (filled white circle, 2.5°) were briefly blinked over the peripheral targets for 0.5 s (cue period). In the ICT, one cue was presented at one of the eight target locations. In the FCT, two identical cues were simultaneously presented at two peripheral locations. After the cues disappeared, the monkey had to maintain fixation for 1.5–3.0 s random length of delay (delay period). At the end of the delay period, the fixation point was turned off, and the monkey was required to make a memory-guided saccade toward the cued location within 0.5 s. The reward was delivered after the monkey maintained fixation on the correct target location for 0.3 s. In FCT trials, a saccade to either of the two locations was regarded as correct. Every correct response was rewarded by a drop of juice, and there was no difference in the amount of reward regardless of the monkey's choice in the FCT or the type of the task.

140 The location of the cue in ICT trials was randomly determined as one of the eight
141 peripheral target locations. Possible cue locations in FCT trials were limited to four
142 locations (0°, 90°, 180° and 270°) to reduce the number of combinations of cue
143 locations. In an FCT trial, cues were presented at two of these four possible locations.
144 Accordingly, trials consisted of eight cue conditions in the ICT and six pair conditions
145 in the FCT. ICT and FCT trials were intermingled in random order.
146 During a recording session, we first presented only ICT trials using the eight
147 possible cue locations as explained above. After we isolated the activity of a single
148 neuron, we examined whether it had a directionally selective task-related activity
149 during performance of the ICT. We collected on average 8.3 trials for each of the eight
150 direction conditions for this screening. We then quantitatively analyzed the activity of
151 the neuron during several task epochs: cue (0–500 ms after the onset of the cue), early
152 delay (0–1000 ms after the start of the delay), late delay (1000–500 ms before the end
153 of the saccade), early response (300–0 ms before the end of the saccade) and late
154 response (0–300 ms after the end of the saccade). If the neuron exhibited a
155 significantly different firing rate during any of these epochs compared to the baseline
156 period (0–1000 ms before the onset of the cue, Dunnett's test for multiple comparisons,
157 $p<.05$), we categorized it as a task-related neuron. The neuron was then further tested
158 for directional selectivity. We used a modified circular normal distribution (von Mises
159 distribution) as a tuning curve to evaluate the modulation of the neuron's firing rate
160 across the eight cue conditions:

$$f(d \mid \mu, \beta, B, R) = B + R \cdot \frac{\exp(\beta \cdot \cos(d - \mu))}{\exp(\beta)}$$

where the firing rate of a neuron (f) was determined as a function of the direction of the cue (*d*), based on the baseline ($0 \leq B$) and magnification (R) factors for the firing rate, and the location (μ) and concentration ($0 \leq \beta$) factors for the von Mises distribution. The peak direction estimated as the μ parameter by fitting of the tuning curve during the epoch in which the firing rate was highest was regarded as the neuron's preferred direction. The size of the receptive field was also quantified from the estimated parameter by $1/\sqrt{\beta}$ which can be regarded as an analog of standard deviation parameter of a normal distribution (σ). If the fitting did not converge, the neuron was considered to lack directional selectivity.

Once the neuron's preferred direction was determined, we rotated the cue locations so that one of the eight possible locations was placed at the neuron's preferred direction. The monkey then performed randomly intermingled ICT and FCT trials using these rotated cue locations. We only used the data recorded in these post-screening trials with rotated cue locations, except for the estimated receptive field of the neurons which was calculated from the activity during screening ICT trials. The four orthogonal cue locations for the FCT are now referred to as T_{in}, T_{ipsi}, T_{contra} and T_{opp}; where T_{in} is the neuron's preferred direction, T_{ipsi} and T_{contra} are the perpendicular directions ipsilateral and contralateral to T_{in}, respectively, and T_{opp} is

180 the opposite direction 180° away from T_{in}. The directions other than T_{in} (i.e., T_{ipsi},
181 T_{contra} and T_{opp}) were also collectively referred to as T_{out}.

182 Since the focus of the present study was to determine how the spatial
183 representation in the PFC was involved in the animal's own decision-making in
184 choosing saccade directions, we only analyzed FCT trials that included T_{in}, where the
185 neuron being recorded was responsible to represent, as one of the two cues. Therefore,
186 only three pair conditions (T_{in} vs T_{ipsi}, T_{in} vs T_{contra}, and T_{in} vs T_{opp}) out of six
187 possible pair conditions were considered in the present analysis. For the ICT, we only
188 used the data for trials in which the visual cue was presented at one of the four
189 locations appeared in the FCT. Each neuron's directional selectivity was confirmed by
190 a post-recording offline analysis as a larger firing rate in T_{in} cue trials than in T_{out} cue
191 trials in the ICT with rotated cue locations (*t*-test, $p<.05$). Neurons that did not show
192 higher activation in T_{in} than in T_{out} cue trials in the ICT were excluded from further
193 analysis.

194 Surgery and Training Procedure

195 We implanted a stainless steel head-holding device and a scleral search coil in the
196 monkeys. A scleral search coil was implanted onto the right eye globe by dissecting
197 the conjunctiva (Judge et al. 1980). The monkeys were first anesthetized by an
198 intramuscular injection of ketamine hydrochloride (10 mg/kg) and then an intravenous
199 injection of pentobarbital sodium (10–15 mg/kg). Heart rate and respiration were

monitored during the surgery. Stainless steel screws were put into the skull to ensure firm adhesion of the head-holding device. The connector for the search coil and the head-holding device were fixed to the skull with dental acrylic. All of the surgical procedures were performed under aseptic conditions.

After the monkeys recovered from surgery, we started training of the tasks. We first trained the monkeys with the ICT. When the monkeys learned to perform the ICT (about 85% correct for more than 5 consecutive experimental sessions), we started to intermingle FCT trials with ICT trials.

After we completed the task training, we performed the second surgery to implant a stainless steel cylinder (MO-903E, Narishige, Tokyo) for the recording of neuronal activity. The monkeys were anesthetized with the same procedure as the first surgery and then fixed to the stereotaxic apparatus. We made a small hole (20 mm in diameter) on the skull with a trephine. The stereotaxic coordination of the center of the hole was set approximately 30.0 mm anterior from the interaural plane and 15.0 mm lateral from the midline, and determined by referring structural magnetic resonance imaging (MRI) pictures of the monkey's brain. We attached the stainless steel cylinder to the hole with stainless steel screws and dental acrylic. All of the surgical procedures were performed under aseptic conditions. After the monkeys recovered from surgery, we started neuronal recordings.

Data Collection

We recorded single-neuron activity from the cortex within and surrounding the principal sulcus. The area of the recording in the lateral PFC was determined based on MRI pictures of the brains. We used glass-coated Elgiloy microelectrodes (0.5–3.0 M at 1 kHz) to record single-neuron activity. An electrode was advanced with a hydraulic microdrive (MO-95, Narishige, Tokyo). Raw neuronal activity was amplified using an amplifier (DAM80, WPI, Sarasota, FL, USA) and monitored on an oscilloscope (SS-7802, IWATSU, Tokyo) and an audio monitor. During experiments, we isolated single-neuron activity from raw activity using a window discriminator (DIS-1, BAK Electronics, Mount Airy, MD, USA) and monitored the isolated single-neuron activity together with raw activity using an oscilloscope. Single-neuron activity and task events were stored as a data file on a laboratory computer.

Data Analysis

All statistical analyses and data-plotting were performed using the statistical software R 3.2.1 (R Core Team 2015). Before testing the difference in central values among groups, we performed Shapiro-Wilk tests to examine normality of the data in each group. We also performed Bartlett's test or Fligner-Killeen test to examine the homogeneity of variances. Based on the results of these tests, we selected nonparametric test when appropriate. We used Holm's correction method for *p*-values on statistical results taken from a set of multiple comparisons unless otherwise noted.

Behavioral Analysis

The proportion correct was calculated separately for the ICT and FCT by dividing the number of trials with correct target capture by the number of trials in which the animal reached the response period.

To examine the animal's preference toward four directions in the FCT, we defined preference indices based on the proportion of chosen direction. For a given direction, we calculated the proportion of trials in which that direction was chosen by the animal from the total number of trials in which that direction was available in the FCT. Calculated four proportions were then divided by their sum. We call these normalized proportions of choosing each direction as preference indices. Preference index was expected to be 0.25 if the animal chose each direction equally in the FCT. Preference indices were separately calculated for the behavior obtained during recordings of each neuron because the absolute angles of the four directions differed based on the location of the receptive field of neurons.

To compare the behaviors in different recording sessions with different cue configurations, we grouped the absolute directions of responses by eight bins of 45° width. Then we averaged the preference indices categorized into each bin. We used the same bins to calculate averaged response times in the ICT and FCT with different response directions. Response times were measured as the latency from disappearance of the fixation point to the onset of a saccade detected by the method in a previous study (Martinez-Conde et al. 2000). We further tested the animal's task performance in

the FCT based on the relative directions from each neuron's receptive fields. For each of the T_{in}, T_{ipsi}, T_{contra} and T_{opp} directions, we calculated the mean response times in correct FCT trials. Response times for these relative directions could vary reflecting the difference in motor execution processes toward different absolute directions. Therefore, for each of the T_{in}, T_{ipsi}, T_{contra} and T_{opp} directions, we also calculated the normalized response times by subtracting the mean response time in the ICT from that in the FCT, and then dividing it by the standard deviation of the response times for that direction in the ICT. This tested whether the animal's speed of responses was different among the four response directions in the FCT, cancelling out the effect of the difference in motor processes for different absolute saccade directions.

Task-Related Activity and ROC Analysis

We used a 100-ms time window sliding in 25-ms steps to make peri-event time histograms to examine task-related activities of the neurons. Constructed histograms were then averaged across neurons to create population histograms. We also used a receiver operating characteristic (ROC) analysis to compare the strength of neuronal activity between two different trial conditions (Britten et al. 1992; Shadlen and Newsome 1996). For each time window, we constructed an ROC curve and calculated the ROC value (area under the ROC curve) using 100 criterion firing rates. To evaluate the onset of ROC elevation, we repeatedly tested the significance of differences in the ROC values of the neurons from 0.5 (one-sample *t*-test, α=.05). If

the ROC values were larger than 0.5 in five consecutive bins, the time of the first bin was regarded as the onset of ROC elevation.

We applied an ROC analysis to the data from both the ICT and FCT. In the ICT, we compared the neuronal firing between T_{in} cue trials and T_{out} cue trials. Therefore, the calculated ROC value is an index of traditional memory-related activity that encoded the spatial location of the cue instructed in that trial. In the FCT, we compared the neuronal firing between T_{in} choice trials and T_{out} choice trials in each pair condition. Therefore, the calculated ROC value is an index of decision-related activity that encoded the subsequently chosen spatial location from the same set of cues.

Baseline Sustainability of Firing

Previous studies have suggested that the dynamics of the spontaneous fluctuation in neural activity reflect the background structural and functional architecture of the network (Tsodyks et al. 1999; Kenet et al. 2003). In the present study, we were particularly interested in the relationship between the persistence of spontaneous activity and the neuron's role in memory and decision-making functions. To quantify the persistence of a neuron's activity at a baseline state, we examined the temporal correlation of firing rates within a trial (Ogawa and Komatsu 2010). We divided the first 800 ms of the pre-cue period (1000–200 ms before cue onset) into eight successive 100-ms time bins. We calculated the trial-to-trial variation in activity within each bin by subtracting the mean firing rate of the given bin across trials from the

301 firing rate for each trial in the same bin. We then calculated the Pearson's correlation
302 coefficient of these values between two different bins interposed by a given length of
303 interval. Seven intervals (0–600 ms in 100-ms steps) were available depending on the
304 combination of the bins, where "0-ms interval" meant two successive bins and
305 "600-ms interval" meant the longest interval between the first and the last bins of the
306 800-ms period used in this analysis. Different pairs of bins with the same interval were
307 pooled to calculate a single correlation coefficient for each interval length. Therefore,
308 seven correlation coefficients were calculated, one for each of the interval lengths, for
309 each neuron. We refer to the calculated correlation coefficient as "baseline
310 sustainability", since it reflects how the activity within a time bin could be sustained
311 until another temporally distant bin.

312 ***Serial Correlation of the Inter-Spike Interval***

313 We also measured the sustainability of the activity of each neuron by calculating a
314 serial correlation of the inter-spike interval (ISI). In this analysis, we first calculated
315 the ISIs of a neuron using all of the collected data including those from non-task
316 epochs such as the inter-trial interval. Next, we calculated Pearson's correlation
317 coefficient between the lengths of successive ISIs. Since the ISI is a measure of the
318 momentary level of activation, a stronger serial correlation of ISI indicates that the
319 activation state once achieved by the neuron tended to persist for a while.

Dimensional Reduction in Population Activity

We used a dimensional reduction technique with a principal component analysis (PCA) to compare the activation patterns of PFC neurons among different task conditions (Briggman et al. 2005; Broome et al. 2006; Churchland et al. 2007; Shenoy et al. 2013). For each neuron, we first calculated the average firing rate in each task condition (four conditions for the ICT and six conditions for the FCT) during ±2000 ms from the cue onset. We used 50-ms time bins sliding in 25-ms steps to calculate the mean firing rates. We then stacked these averaged firing rates for each neuron and each condition into an M×N matrix, where M is the number of bins in a trial multiplied by 10 (total number of task conditions) and N is the number of neurons under interest. We applied a PCA to this matrix. The first three principal components were used to create the principal component state space. The activation state and its transition were represented as a trajectory inside the state space. To evaluate how the neuronal activation patterns differed between the conditions, we calculated the Euclidean distances between trajectories.

Correlation Analysis between Tasks

To investigate how spatial representation was constructed in the network of PFC neurons during an FCT trial, we applied a correlation analysis to the activation patterns of PFC neurons in different tasks. In this analysis, we tested the similarity of the neuronal activation patterns during the FCT to those at the end of the delay period of the ICT. At the end of the delay period in an ICT trial, spatially selective PFC neurons

were expected to represent a sole spatial location to which a saccade was going to be directed soon thereafter. Therefore, the activation pattern of PFC neurons in this period could be regarded as a built template when the network had already finished representing a single spatial location. On the other hand, the pattern of neuronal activation in the cue period of an FCT trial should be more ambiguous because two spatial locations are represented in the network. As the delay period progressed in an FCT trial, the activation pattern should gradually become similar to that in the ICT, since the monkey was required to prepare a saccade toward only one of the two locations. By testing how the neuronal activity was similar between these different periods in different tasks, we tried to examine how the spatial information needed for a subsequent saccade was constructed from the two locations presented in the FCT.

For the ICT, we used a 500-ms time bin in a pre-response period ranging from -1000 to -500 ms from the end of the saccade. For the FCT, we used 250-ms time bins sliding through a trial in 1-ms steps. In a given time bin, we first calculated each neuron's average firing rates in each task condition. We then subtracted each neuron's grand average firing rate among task conditions in that bin from its firing rates in each task condition, which gave the discrepancies of each neuron's firing rates in different conditions from its average. Finally, we calculated the rank correlation (Kendall's tau) between each time bin of the FCT and the pre-response period of the ICT between task conditions in which the monkey made the same response (e.g., T_{ipsi} cue trials in the ICT and T_{out} choice trials in the T_{in} vs T_{ipsi} pair condition in the FCT). To evaluate

362 the onset of significant correlation, we tested the significance of the correlation in each
363 bin with α=.05. If there was a significant correlation between the FCT and
364 pre-response period activity in the ICT, and if the correlation remained significant
365 until the last time bin of the peri-cue period in the FCT, we regarded the onset of the
366 first bin of these periods as the onset of significant correlation.

367 We also examined the correlation between the activation patterns in T_{out} choice
368 trials in the FCT and those in T_{in} cue trials in the ICT. These trial conditions differed
369 with respect to the final saccade direction, and thus were expected to result in different
370 activation patterns of directionally selective PFC neurons.

371 # Results

372 ## Behavioral Performance

373 We analyzed the behavioral performance of the animals during the recording sessions.
374 The average proportion of correct performance in the ICT and FCT was 98.0% and
375 98.3% for monkey O and 99.8% and 99.9% for monkey E, respectively. There was no
376 statistically significant difference in task performance between the ICT and FCT in
377 either monkey (paired *t*-test, corrected p = .50 and .13). In correct ICT and FCT trials,
378 the mean response time from the disappearance of the fixation point to the onset of a
379 saccade was 263 ms and 265 ms for monkey O and 231 ms and 232 ms for monkey E,

respectively. There was also no significant difference in the response time between the tasks (paired *t*-test, corrected $p = .42$ and .50).

We further examined the relationship between the animals' behavior and response directions in the tasks. Figure 1b shows the response times (lines) and preference indices (bars) for each direction. Two-way ANOVA on each animal's response times revealed a significant main effect of direction (uncorrected $p<.001$ for both monkeys), but there were no main effect of the type of the tasks (uncorrected $p = .12$ and .24 for monkey O and E, respectively) nor the interaction between task and direction (uncorrected $p = .70$ and .35). In addition, there was no significant effect of direction on the preference indices calculated from the proportion of choices for each direction in the FCT (one-way ANOVA, uncorrected $p = .13$ and .10). Therefore, the observed difference in response times for each direction were more likely to be attributed to the difference in motor execution process rather than the effect of the animal's unequivalent motivation for responses toward each direction.

Neuronal Database

We recorded neurons in and around the principal sulcus during performance of the tasks. Out of 444 neurons recorded, 107 exhibited directionally selective activation during at least one epoch in the screening ICT trials. These neurons were further recorded in randomly intermingled ICT and FCT trials with rotated cue locations (see Tasks in Materials and Methods section). Eighty-four neurons had at least five correct trials for each of the six FCT conditions (three pair conditions × two choice results)

and were confirmed to have directional selectivity in the post-recording offline analysis. We used these neurons for further analysis. We only used the activity of PFC neurons recorded during intermingled ICT and FCT trials for the analysis below.

Based on the rotated cue locations (T_{in}, T_{ipsi}, T_{contra} and T_{opp}) determined by the receptive field of each neuron, we further tested the animals' task performance in the FCT for each direction (Fig. 1c). There was no difference in the proportion of T_{in} choice in all the three pair conditions (one-way ANOVA, $p = .11$). The proportion of T_{in} choice was not significantly different from 0.5 (one-sample Wilcoxon rank sum test, corrected $p>.05$ for all the pair conditions). Also, there was no difference in the response times (one-way ANOVA, $p = .11$) and the normalized response times (Kruskal-Wallis test, $p = .11$) for each response direction. The normalized response times were not significantly different from 0 (one-sample Wilcoxon rank sum test, corrected $p>.05$ for all the directions), meaning that the responses toward each of the four relative directions in the FCT were comparable to those to the same direction in the ICT. These results indicate that observed characteristics in neuronal activity reported below could not be attributed to the animal's preference toward a particular direction nor to the difference in the degree of motor preparation toward each direction.

Choice-Predictive Activity

Figure 2 shows the activity of two representative neurons. Both neurons exhibited a larger firing rate in T_{in} than in T_{out} cue trials (*t*-test, 0–500 ms from cue onset, $p<.05$) during the cue period of the ICT (top row: ICT trials). Thus, they were more activated during the cue period when the visual cue was presented at T_{in}. We examined whether the activity of these neurons was related to the monkey's choice in the FCT (bottom three rows: FCT trials for three pair conditions that included T_{in}). The neuron shown in Fig. 2a exhibited activation in response to the presentation of cues in FCT trials. The magnitude of cue-period activity was almost identical in trials in which the monkey chose T_{in} (T_{in} choice trials) and trials in which the monkey chose T_{out} (T_{out} choice trials). This is not surprising because one of the two cues was always presented at the T_{in} location (neuron's preferred direction) in all of these three pair conditions. Therefore, this neuron was likely to exhibit a similar magnitude of cue-period activity when the visual cue was presented at T_{in} regardless of whether the monkey was going to choose T_{in} or T_{out} later in that trial.

The other neuron in Fig. 2b showed cue-period activity that was related to the animal's subsequent choice in the FCT. In all three pair conditions, the strength of the transient response to the same two cues was significantly different depending on the monkey's subsequent choice. While the neuron was strongly activated during the cue period in T_{in} choice trials, this activation was not observed in T_{out} choice trials, even

though one of the cues was simultaneously presented at T_{in} (*t*-test between T_{in} and T_{out} choice trials, 0–500 ms from cue onset, $p<.05$, pair conditions collapsed). We refer to this firing pattern of PFC neurons (i.e., strong activation in T_{in} choice trials compared to T_{out} choice trials in the FCT) as "choice-predictive". In every FCT trial with a given pair condition, the monkey was presented with two physically identical cues at the same spatial locations regardless of which of them was chosen later in that trial. Therefore, choice-predictive activity can not be explained as a mere reflection of the physical stimuli. Rather, the strong correlation between neuronal activity and the animal's subsequent choice suggests that PFC neurons play an active role in the free choice of a spatial location. Choice-predictive activity was also observed in the pre-cue period (Fig. 2b). The activity of the neuron was slightly, but significantly, higher before the start of the cue period when the monkey was going to choose the neuron's preferred direction in the current trial (*t*-test between between T_{in} and T_{out} choice trials, 1000–0 ms before cue onset, $p<.05$, pair conditions collapsed).

Population Activity

We confirmed the presence of choice-predictive activity in the cue and pre-cue periods of the FCT in a population analysis. Figure 3 shows population histograms and ROC transition of 59 PFC neurons that exhibited directionally selective cue-period activity. Differential firing in response to the cues presented in the FCT was consistently observed between T_{in} choice trials and T_{out} choice trials (Fig. 3b). We analyzed the

activity of these neurons during the cue period in each task condition (0–500 ms from cue onset). In the ICT, cue-period activity in T_{in} trials (average 20.2 spikes/s) was significantly stronger than that in T_{ipsi} (12.0 spikes/s), T_{contra} (11.6 spikes/s) and T_{opp} (9.8 spikes/s) trials (paired *t*-test, corrected $p<.001$ for all comparisons). In the FCT, cue-period activity in T_{in} choice trials was also significantly stronger than that in T_{out} choice trials in all three pair conditions (corrected $p<.001$ for all pair conditions). In comparisons of different FCT pair conditions, the activity in T_{in} choice trials were comparable among the T_{in} vs T_{ipsi} (19.4 spikes/s), T_{in} vs T_{contra} (20.2 spikes/s) and T_{in} vs T_{opp} (20.6 spikes/s) pair conditions (corrected $p=.94$, .89 and .94, respectively). However, in the T_{out} choice trials, neurons tended to be more activated in the T_{in} vs T_{ipsi} pair condition (16.9 spikes/s) than in the T_{in} vs T_{contra} (14.9 spikes/s, corrected $p=.060$) and T_{in} vs T_{opp} (14.9 spikes/s, corrected $p=.065$) pair conditions, while there was no significant difference between the latter two pair conditions (corrected $p=.97$).

We also performed an ROC analysis on the cue-period activity of these neurons in T_{in} and T_{out} choice trials in the FCT. In all the three pair conditions, average ROC values (0.57, 0.61 and 0.63 for each of the three pair condition) were all significantly larger than 0.5 (one-sample *t*-tests, corrected $p<.001$ for all of the conditions) in the cue period (0–500 ms from cue onset). By examining the change in the ROC value throughout the entire trial epoch using a sliding window, we observed early elevation of the ROC value that started before the presentation of the cues (Fig. 3d). A

479 significant increase in the ROC value from 0.5 was observed 750 ms before the onset
480 of the cues. The same analysis of activation during the ICT revealed that an elevation
481 of the ROC value (calculated between the T_{in} and T_{out} cue trials) was observed 150
482 ms after the onset of the cue when the direction of the saccade was instructed (Fig. 3c).
483 These results indicate that the choice-predictive activity of PFC neurons in the pre-cue
484 period of the FCT was not an artifact of the task structure, but rather reflected the
485 influence of these neurons on the animal's decision-making regarding the saccade
486 direction when the choice was left to the animal.

487 Relationship between Choice-Predictive Activity and
488 Persistent Delay-Period Activity

489 To further investigate the role of PFC neurons in the decision-making regarding the
490 saccade direction, we compared the activities and firing properties of neurons with and
491 without choice-predictive activity in the FCT. We categorized a neuron as
492 choice-predictive if it exhibited a differential activation between the T_{in} and T_{out}
493 choice trials during the cue and pre-cue periods (-1000 to 500 ms from cue onset) in at
494 least one of the three FCT pair conditions (*t*-test). Figure 4 shows population
495 histograms of neurons with and without choice-predictive activity. PFC neurons with
496 choice-predictive activity also showed directionally selective persistent delay-period
497 activity. On the other hand, neurons without choice-predictive activity were activated
498 only during cue presentation, and did not exhibit persistent delay-period activity.

Based on this difference in task-related activity between neurons with and without choice-predictive activity, we further compared these two groups in terms of the persistence of activation (Fig. 5). We first quantified the strength of directionally selective persistent activity during the delay period of the ICT for each neuron by calculating the ROC value between T_{in} and T_{out} cue trials at the middle of the delay (1000–1500 ms from the start of the delay period of the ICT). When compared among all of the directionally selective neurons (Fig. 5a, n = 84), the strength of directionally selective persistent activity in the ICT was closely correlated (Pearson's R=.345, p<.001) with the strength of the choice-predictive difference in activity in the cue and pre-cue periods of the FCT (quantified by the ROC value calculated between T_{in} and T_{out} trials within -1000 to 500 ms from cue onset, pair conditions collapsed). When compared between groups, choice-predictive neurons had stronger directional selectivity in the delay period in the ICT than choice-unpredictive neurons (Fig. 5c, Wilcoxon rank sum test, p<.001). In addition, the choice-predictive neurons showed a higher baseline sustainability of activation even in the pre-cue period (Fig. 5d, t-test, p<.05) and a stronger serial correlation of the ISI (Fig. 5e, Wilcoxon rank sum test, p<.05). Choice-predictive neurons were characterized by a higher sustainability of activation even between temporally distant time bins (Fig. 5b). The persistence of activation as measured by the baseline sustainability and the serial correlation of the ISI could be important for retention of the spatial information as sustained firing during the delay, and thus can be regarded as a key feature of PFC neurons in spatial

working memory function. The coupling of these measures to the presence of choice-predictive activity in the early task epochs of the FCT suggests that the firing properties of PFC neurons that are essential to the memory function might also lead to a distinctive role of these neurons in the selection of spatial locations in a free-choice condition.

We examined the possible effect of behavioral difference as well as the difference in receptive field properties between choice-predictive and unpredictive neurons. However, there were no difference between the two groups of neurons in the distribution of the preferred directions (Fig. 5f, Watson's test for homogeneity of circular data, $p>.10$) nor the size of the receptive fields (Fig. 5g, Wilcoxon rank sum test, $p = .21$). Also, two-way ANOVA on the proportion of T_{in} choices revealed no main effects of neuron groups (choice-predictive/unpredictive neurons) and pair conditions, nor the interaction of these two factors (Fig. 5h, $p>.05$ for both main effects and the interaction). One-sample *t*-tests revealed that the proportion of T_{in} choices was not significantly different from 0.5 in any of the neuron groups and pair conditions (corrected $p>.05$ for all the 2×3 combinations of neuron groups and pair conditions). The same comparison on the difference of the response times between T_{in} choice and T_{out} choice trials also revealed no significant main effects nor interaction of neuron groups and pair conditions (Fig. 5i, $p>.05$ for both main effects and the interaction). One-sample *t*-tests revealed that the difference of the response times between T_{in} choice and T_{out} choice trials was not significantly different from zero in

any of the neuron groups and pair conditions (corrected p>.05 for all the combinations).

Comparison of the Neuronal Activation Pattern in a State Space

To gain further insight into how spatial representations are held and integrated in the network of the PFC to perform a final saccadic response in the FCT, we used a dimensional reduction technique. The change in neuronal activation in each task condition in the ICT and FCT was expressed as a trajectory in a principle component state space (Fig. 6). In the ICT (Fig. 6a), the four trajectories that represented the neuronal activation patterns in T_{in}, T_{ipsi}, T_{contra} and T_{opp} cue trials remained within the neighboring area until the time of cue onset. The trajectory for T_{in} cue trials then started to diverge from those for the other three cue conditions, which reflected a strong transient activity of directionally selective neurons in response to cue presentation (Fig. 3a). In the FCT (Fig. 6b), the trajectories for T_{in} choice and T_{out} choice trials reached slightly distant points in the space even at the beginning of the cue period. After the presentation of the cues, the trajectories for T_{in} choice trials further deviated from those for T_{out} choice trials and tracked similar paths to the trajectory for T_{in} cue trials in the ICT. Conversely, the trajectories for T_{out} choice

559 trials returned to the initial state during the cue and delay periods, in a similar manner
560 to T_{out} cue trials in the ICT.

561 However, in the T_{in} vs T_{ipsi} pair condition, the trajectory for T_{out} choice trials
562 remained relatively adjacent to that for T_{in} choice trials, compared to the other two
563 pair conditions. To evaluate the difference in neuronal activation patterns, we
564 calculated the distance between the trajectories for the T_{in} choice and T_{out} choice trials
565 in each of the three pair conditions in the FCT (Fig. 6c). In the T_{in} vs T_{contra} and T_{in}
566 vs T_{opp} pair conditions, the distance between the trajectories for T_{in} choice and T_{out}
567 choice trials increased in the cue period. In the T_{in} vs T_{ipsi} pair condition, the distance
568 between T_{in} and T_{out} choice trials remained relatively small in the cue period and
569 gradually increased during the delay period. The average distance between T_{in} and
570 T_{out} trajectories during the cue period was 24.7, 66.5 and 72.8 for the T_{in} vs T_{ipsi}, T_{in}
571 vs T_{contra}, and T_{in} vs T_{opp} pair conditions, respectively. Paired *t*-tests revealed that
572 there was a significantly less distance between the trajectories for T_{in} and T_{out} choice
573 trials in the T_{in} vs T_{ipsi} pair condition than in the other two pair conditions (corrected
574 $p<.001$). The distance between the T_{in} and T_{out} trajectories was also greater in the T_{in}
575 vs T_{opp} pair condition than in the T_{in} vs T_{contra} condition (paired *t*-test, corrected
576 $p<.001$), but this difference was small. These results support the observation in the
577 population histograms and ROC analysis that choice-predictive activity was

established more slowly when the two cues were presented in the same hemifield (T_{in} vs T_{ipsi} pair condition).

Effect of Cue Configuration

Previous analyses suggested that the time course of the establishment of choice-predictive activity was dependent on the configuration of the cues. To investigate how the final spatial representation was constructed in each pair condition of the FCT, we used a between-task correlation analysis on the firing patterns of directionally selective PFC neurons. In this analysis, we examined the correlation of neuronal activity between the FCT and the pre-response period of the ICT. For each task condition and each time bin in the FCT, we calculated the correlation coefficient between the activation of directionally selective PFC neurons (n = 84) in that time bin and that in the pre-response period (1000–500 ms before the end of the saccade) of the ICT. As the decision-making process regarding the subsequent saccade direction progressed in the FCT, the correlation coefficient was expected to increase because the activation pattern of PFC neurons should have been similar to that when the animal was ready to make a saccade in the ICT. By measuring the transition of correlation coefficients in each task condition, we tried to clarify how the configuration of the cues might influence the dynamics of visuospatial decision-making in FCT trials.

Figure 7 shows the correlation in the neuronal activation pattern between the FCT and the pre-response period of the ICT. We first examined the correlation between the

598 ICT and FCT in which the monkey eventually made a response to the same direction
599 (correlation between T_{in} cue/choice trials for Fig. 7a, T_{out} cue/choice trials for Fig. 7b).
600 In the T_{in} vs T_{contra} and T_{in} vs T_{opp} pair conditions, the correlation coefficients started
601 to rise from zero at around the beginning of the cue period. In the T_{in} vs T_{contra} pair
602 condition, a significant correlation started to be observed 142 ms before the start of the
603 cue period in T_{in} choice trials, and 48 ms after cue onset in T_{out} choice trials. In the
604 T_{in} vs T_{opp} pair condition, a significant correlation started to be observed 90 ms before
605 and 113 ms after cue onset in T_{in} choice and T_{out} choice trials, respectively. However,
606 in the T_{in} vs T_{ipsi} pair condition, the development of a correlated activation pattern
607 was weak. In T_{in} choice trials, the onset of significant correlation was 408 ms after cue
608 presentation. In T_{out} choice trials, significant correlation that lasted stably during the
609 delay period was not observed. This result indicates that, in the network of spatially
610 selective PFC neurons, a sole spatial representation was constructed from the
611 presented two locations more slowly when the two cues were located in the same
612 hemifield, consistent with the observation in the previous analyses on population
613 activity (Fig. 3d) and the neuronal state space (Fig. 6c). Especially, the slower
614 development of choice-predictive activity in the T_{in} vs T_{ipsi} pair condition may be the
615 result of the disarranged construction of spatial representation in T_{out} choice trials in
616 this pair condition.

For T_{out} choice trials in the FCT, we also examined the correlation of the neuronal activation pattern with that in T_{in} cue trials in the ICT (Fig. 7c). In all three pair conditions of the FCT, T_{in} cue was presented during the cue period. However, since the final saccade directions were not in the neurons' receptive fields in T_{out} choice trials, the activity of PFC neurons were expected to gradually become different compared to when T_{in} was instructed in the ICT. We confirmed this prediction as an early negative correlation of the neuronal activation patterns in the T_{in} vs T_{contra} and T_{in} vs T_{opp} pair conditions. In T_{out} choice trials, the population activity of PFC neurons started to differ from that in T_{in} cue trials in the ICT at 296 ms and 158 ms before the onset of the cues in the T_{in} vs T_{contra} and T_{in} vs T_{opp} pair conditions, respectively. In contrast, the onset of a significant negative correlation was 941 ms after cue onset (441 ms after the start of the delay period) in the T_{in} vs T_{ipsi} pair condition. This means that the activation state of PFC neurons in T_{out} choice trials in the T_{in} vs T_{ipsi} pair condition remained indistinguishable from that in T_{in} cue trials in the ICT for a longer period. This result also suggested that the construction of spatial representation for T_{out} was slower in the T_{in} vs T_{ipsi} pair condition than in the other pair conditions.

Discussion

In the present study, we investigated the role of spatially selective PFC neurons in animal's decision about saccade direction in a free choice condition. When T_{in} was later chosen as a saccade direction, PFC neurons were strongly activated by cue presentation despite the presence of another cue outside their preferred direction. Choice-predictive activity was distinct from the very beginning of the cue period and was observed even before cue onset.

The positive correlation between the strength of the delay-period activity in the ICT (memory-related activity) and the strength of the choice-predictive activity in the cue and pre-cue periods of the FCT (decision-related activity) revealed that PFC neurons with stronger memory-related activity in the ICT tended to show stronger choice-predictive activity in the peri-cue periods of the FCT. The stronger sustainability of firing in neurons with choice-predictive activity suggested that memory and decision functions are supported by a common feature of PFC neurons to sustain their activation state within the circuitry. In addition, when to-be-chosen T_{out} was located in a hemifield different from that in which T_{in} was located, the transient response to cue presentation was weak. However, when to-be-chosen T_{out} was in the same hemifield as T_{in}, the cue-period activity was stronger, even though the neuron's preferred direction was not going to be chosen. This indicates that unnecessary spatial information tended to be suppressed from the beginning of its representation in the

PFC, but this adaptive modulation was modest if the two spatial locations were in the same hemifield. Our present study revealed that the role of the PFC in decision-making process is closely linked to its role in information maintenance process, and these different processes share the same functional characteristics that emerged from the underlying cellular mechanism.

Activity of PFC Neurons Related to the Animal's Decision

In the present study, we found that the strength of neurons' activity in pre-cue and cue periods was correlated with the animal's subsequent decision regarding the saccade direction (choice-predictive activity). However, in the FCT, one of the six pair conditions was randomly assigned in each trial. Also, FCT trials were randomly intermingled with ICT trials. Only after cue presentation could the animal know whether they were allowed to choose the saccade direction by themselves or where the options for the choice would be. Therefore, it was impossible for the animal to make a reasonable decision before cue onset. We propose that this early choice-predictive activity can be explained as an influence of fluctuating neuronal firing before the start of a trial. In each trial, the activity of directionally selective neurons can randomly fluctuate during the pre-cue period. This fluctuation of activity can be regarded as baseline random noise in spatial representation in the PFC. If the activity of neurons that are responsible for a particular direction happen to be elevated during the pre-cue period of an FCT trial, these neurons should be able to more quickly respond to the presentation of cues one of which appeared at their preferred direction. In the network

675 of the PFC, neurons responsible to different spatial locations have inhibitory
676 connections, so that the PFC retains only the most relevant spatial information in a
677 winner-take-all manner (Rao et al. 1999; Compte et al. 2000; Wang et al. 2004).
678 Therefore, the faster construction of a spatial representation will disturb the formation
679 of other spatial representations through mutual competition, resulting in the adoption
680 of the prematurely biased location as the direction of the saccade in the current trial.
681 As a result, trials in which directionally selective PFC neurons show slightly stronger
682 activation before the cue period should be over-represented among trials in which their
683 preferred direction was later chosen by the animal.

684 Previous studies have reported the activity of neurons in the PFC, frontal eye field,
685 supplemental eye field and lateral intraparietal cortex using memory-guided
686 (Watanabe et al. 2006; Watanabe and Funahashi 2007) or visually guided (Coe et al.
687 2002) free choice tasks. However, in these studies, a same set of fixed locations were
688 repeatedly presented in a block of trials. Therefore, a detailed investigation of the time
689 course of neuronal activity and the interpretation of its role in decision-making were
690 difficult since the animal could easily predict the available options independently of
691 the progress of a trial. Also, in those task setups, the animal could exhibit a strong
692 tendency or strategy to repeatedly choose the same option. Therefore, the previous
693 studies used particular reinforcement rules to prohibit the animal from choosing the
694 same option repeatedly, and forced the animal to choose different options. This
695 procedure can be regarded as a trained allocation of choices administrated by a reward

696 schedule. In the present study, we intermingled ICT and FCT trials and changed the
697 combination of the options for a decision. In addition, the absolute locations of the
698 four options changed randomly for the animal depending on the receptive field of the
699 neuron. As a result, the monkeys were presented with different decision contexts from
700 trial to trial, and their choices were substantially varied among options without
701 restrictive rules for decision. We propose that our current experimental design is more
702 appropriate for the investigation of the neuronal mechanisms of internally driven
703 decision-making compared to the previous studies.

704 In other cortical areas, a biasing effect of baseline fluctuation of the neuronal
705 activity on the subsequent animal's behavior has been reported (Platt and Glimcher
706 1999; Shadlen and Newsome 2001). For example, Shadlen and Newsome (2001)
707 reported that the activity of primate lateral intraparietal neurons before the onset of
708 random-dot motion stimulus was higher when motion coherency was weak and the
709 neurons' preferred motion direction was going to be chosen. They argued that this was
710 because the existing neuronal fluctuation before stimulus presentation biased the
711 subsequent competition between the representations of different motion directions.
712 Rolls and Deco (2011) recently reported that this kind of bias based on random
713 fluctuation could actually take place in an integrate-and-fire attractor network model.
714 They confirmed the relationship between pre-existing random fluctuation in
715 spontaneous activity and the result of the subsequent neuronal competition in an
716 artificial network in which there was no potential confounding such as a subject's

specific behavioral strategies. Our present results are in accord with these previous reports.

Relationship between Decision-Making and Memory Maintenance

We found that neurons with choice-predictive activity during cue and pre-cue periods showed higher sustainability of firing such as an elevated delay-period activity (Fig. 4 and 5). The persistent delay-period activity of PFC neurons while the monkey is remembering a particular spatial location is thought to be the neural basis of spatial working memory (Funahashi et al. 1989, 1990; Goldman-Rakic et al. 1990; Miller and Cohen 2001; Fuster 2008). An elevated firing rate sustained during several seconds of delay is not likely to be supported only by subcellular mechanisms, and is instead attributed to the network property of the PFC with recurrent feedback inputs (Constantinidis and Wang 2004; Wang 2013). We propose that the strong correlation between memory-related activity (persistent delay-period activity in the ICT) and decision-related activity (choice-predictive activity in the FCT) is a consequence of this network property of the PFC. Since PFC neurons are mutually interconnected, the incidental activation of a group of neurons before the start of a trial could persist for some time through this network. Heterogeneity in the activation level among neurons might further be amplified during the pre-cue period through mutual facilitation and competitive inhibition of neurons with the same and different directional selectivities,

737 respectively. The premature imbalance of activation will then result in a difference in
738 the strength of cue representations in the cue period and the animal's final choice
739 toward the strongly represented direction in the FCT.

740 In recent electrophysiological research, there has been a debate about the role of
741 the lateral PFC in spatial information processing. Several studies have proposed that
742 lateral PFC is more related to the spatial attention than spatial working memory
743 (Lebedev et al. 2004; Messinger et al. 2009; Everling et al. 2002; DeSouza and
744 Everling 2004; Lennert and Martinez-Trujillo 2011, 2013; Tremblay et al. 2015). For
745 instance, by using a behavioral task in which a location to remember and a location to
746 allocate a visually-guided attention are separated, Lebedev et al. (2004) showed that
747 large proportion of lateral PFC neurons are selective to attended rather than
748 remembered spatial location. In their study, spatial working memory process was
749 depicted as maintenance memory, and separated from attention process by preventing
750 the animal from paying attention to the remembered location. However, the concept of
751 working memory includes both active maintenance and manipulation of information
752 (Baddeley and Hitch 1974; Baddeley 1986, 2003). Working memory tasks in animals
753 (Dudchenko 2004) and humans (Miyake et al. 2000) typically consist of attentional
754 shifting, updating or inhibitory control of the maintained information. This is because
755 a mere maintenance of information is unlikely in a variety of cognitive operations, and
756 the maintenance of task-relevant information necessarily requires attentional control.
757 This joint formularization of memory and attention is the essence of the working

758 memory, and the validity of working memory concept in clinical, developmental and
759 experimental psychology (Baddeley 2003; Saperstein et al. 2006; Conway et al. 2003;
760 Kane and Engle 2003) suggests that maintenance and attentional manipulation of
761 information can not be dissociated as independent processes.

762 Based on these psychological backgrounds, the elucidation of how maintenance
763 and manipulation of information are simultaneously and jointly performed in the
764 activity of cortical neurons is essential for the understanding of the neuronal
765 mechanism of working memory. Therefore, in the present study, we used a traditional
766 memory-guided saccade task combined with subjective decision-making process. As a
767 result, we observed that fluctuation of the activity of PFC neurons before cue
768 presentation induced an early bias in the representation of spatial cues, and eventually
769 influenced the animal's decision. Importantly, this task-related activity was correlated
770 with more fundamental firing characteristic of PFC neurons to sustain its activation
771 state for relatively longer period. If there is no such persistence in neuronal activity,
772 the premature fluctuation of activity before a trial could not survive until presentation
773 of the cues and should never influence the animal's behavior. In this sense, the
774 capability of the PFC network to maintain spatial information played a pivotal role in
775 the decision-making process under a free-choice condition. This is a succinct example
776 that the network property of the PFC that enables the maintenance of information can
777 be regarded as a key feature in understanding the PFC's roles in other cognitive
778 processes (Procyk and Goldman-Rakic 2006; Wang 2008). Especially, the effect of

pre-existing neural state on subsequent decision-making is a prevailing subject in recent noninvasive electrophysiological studies in human (Hesselmann et al. 2008; Bode et al. 2012; Bengson et al. 2014). Our present report directly demonstrated the neuronal underpinning of such phenomena from the viewpoint of the known function and characteristics of PFC neuron's activity, and also showed that the influence of pre-existing fluctuation takes place in the order of hundreds milliseconds in task-related neuronal activity. Our report provides a clue for integrated understanding of lateral PFC's role in spatial decision-making and working memory functions, from a viewpoint of basic characteristics of neuronal firing in this cortical area.

Competition of Spatial Representations Within or Between Hemifields

In previous studies regarding the role of the PFC in working memory function, a single visual cue has been used to inform the animals of the location to be remembered for an upcoming saccade (Boch and Goldberg 1989; Funahashi et al. 1989, 1990; Rainer et al. 1998). In these studies, PFC neurons with mnemonic visuospatial activity tended to have directional selectivity toward locations contralateral to the side of the hemisphere being recorded. A unilateral lesion to the PFC was reported to result in disrupted performance of the memory-guided saccade to the contralateral hemifield (Funahashi et al. 1993a). These findings suggest that the PFC is organized to participate in the processing of spatial information in the contralateral hemifield (Funahashi 2013).

799 The activity of PFC neurons during the performance of a memory-guided saccade
800 task in which the monkeys chose the saccade direction by themselves has been
801 previously reported (Watanabe et al. 2006; Watanabe and Funahashi 2007). However,
802 in those experiments, the locations of the cues were fixed to the four perpendicular
803 directions and all the four cues were repeatedly presented in a block of trials.
804 Therefore, the influence of contralateral organization of the PFC on the representation
805 of multiple pieces of spatial information could not be examined. In the present study,
806 we compared the time course of the emergence of choice-predictive activation among
807 the three FCT pair conditions. We found that choice-predictive activity developed
808 more slowly in the T_{in} vs T_{ipsi} pair condition than in the T_{in} vs T_{contra}/T_{opp} conditions
809 (Fig. 6). The slow construction of the final spatial representation was especially
810 obvious in T_{out} choice trials in the T_{in} vs T_{ipsi} pair condition (Fig. 7). We propose that
811 this stronger representation of the unchosen direction when the two cues are located in
812 the same hemifield is the result of the contralateral organization of the PFC. Since
813 neurons with directional selectivity toward a particular side of the visual space are
814 assembled in the contralateral hemisphere of the PFC, they may be more tightly
815 interconnected through local circuits than neurons with preferences for different
816 hemifields, which are more likely to be distributed in different hemispheres and thus
817 require callosal connections to interact with each other. A recent study on the
818 concurrent memorization of multiple spatial locations has also suggested a stronger
819 interaction between spatial representations within the same hemifield (Matsushima and

820 Tanaka 2014). Through this stronger local connection, the spontaneous fluctuation of
821 neuronal activity can be more frequently shared by neurons with a preference for the
822 same hemifield. The shared fluctuation between neurons before the start of a trial can
823 be regarded as unbiased pre-existing spatial representation, which leads to strong
824 representations of both subsequently chosen and unchosen locations in response to the
825 presented cues. In contrast, the pre-existing activation levels may vary between
826 neurons with preferences for locations in different hemifields, which can then cause
827 suppression of the representation of the subsequently unchosen location by amplifying
828 the premature bias. Therefore, the difference in the time course of the development of
829 choice-predictive activity among pair conditions can be explained by uneven
830 lateralization of directionally selective neurons in the PFC. Future studies with
831 simultaneous recordings of PFC neurons are needed for quantitative investigation of
832 correlated fluctuation in the spontaneous activity of spatially selective neurons.

833 # Grants

834 This research was supported by Grants-in-Aid for Scientific Research (21240024 and
835 25240021) from the Ministry of Education, Culture, Sports, Science and Technology
836 (MEXT) of Japan to S. F., and by a Grant-in-Aid for JSPS Fellows (23·7155) from the
837 Japan Society for the Promotion of Science to K. M. The animals were provided by the
838 National BioResource Project “Japanese Monkeys” supported by the MEXT, Japan.

Disclosures

There are no competing financial interests.

References

Baddeley A. *Working Memory*. Oxford, UK: Oxford University Press, 1986.

Baddeley A. Working memory: looking back and looking forward. *Nat Rev Neurosci* 4: 829–839, 2003.

Baddeley AD, Hitch G. Working memory. In: *Recent Advances in Learning and Motivation.*, edited by Bower GH, New York: Academic Press, 1974, volume 8 of *Psychology of Learning and Motivation*, pp. 47–89.

Bengson JJ, Kelley TA, Zhang X, Wang JL, Mangun GR. Spontaneous neural fluctuations predict decisions to attend. *J Cogn Neurosci* 26: 2578–2584, 2014.

Boch RA, Goldberg ME. Participation of prefrontal neurons in the preparation of visually guided eye movements in the rhesus monkey. *J Neurophysiol* 61: 1064–1084, 1989.

Bode S, Sewell DK, Lilburn S, Forte JD, Smith PL, Stahl J. Predicting perceptual decision biases from early brain activity. *J Neurosci* 32: 12488–12498, 2012.

Briggman KL, Abarbanel HDI, Kristan WB. Optical imaging of neuronal populations during decision-making. *Science* 307: 896–901, 2005.

Britten KH, Shadlen MN, Newsome WT, Movshon JA. The analysis of visual motion: a comparison of neuronal and psychophysical performance. *J Neurosci* 12: 4745–4765, 1992.

Broome BM, Jayaraman V, Laurent G. Encoding and decoding of overlapping odor sequences. *Neuron* 51: 467–482, 2006.

Churchland MM, Yu BM, Sahani M, Shenoy KV. Techniques for extracting single-trial activity patterns from large-scale neural recordings. *Curr Opin Neurobiol* 17: 609–618, 2007.

Coe B, Tomihara K, Matsuzawa M, Hikosaka O. Visual and anticipatory bias in three cortical eye fields of the monkey during an adaptive decision-making task. *J Neurosci* 22: 5081–5090, 2002.

Compte A, Brunel N, Goldman-Rakic PS, Wang XJ. Synaptic mechanisms and network dynamics underlying spatial working memory in a cortical network model. *Cereb Cortex* 10: 910–923, 2000.

Constantinidis C, Franowicz MN, Goldman-Rakic PS. Coding specificity in cortical microcircuits: a multiple-electrode analysis of primate prefrontal cortex. *J Neurosci* 21: 3646–3655, 2001a.

Constantinidis C, Franowicz MN, Goldman-Rakic PS. The sensory nature of mnemonic representation in the primate prefrontal cortex. *Nat Neurosci* 4: 311–316, 2001b.

Constantinidis C, Wang XJ. A neural circuit basis for spatial working memory. *Neuroscientist* 10: 553–565, 2004.

Conway ARA, Kane MJ, Engle RW. Working memory capacity and its relation to general intelligence. *Trends Cogn Sci* 7: 547–552, 2003.

874 Courtney SM, Petit L, Maisog JM, Ungerleider LG, Haxby JV. An area specialized for spatial working
875 memory in human frontal cortex. *Science* 279: 1347–1351, 1998.

876 DeSouza JFX, Everling S. Focused attention modulates visual responses in the primate prefrontal cortex.
877 *J Neurophysiol* 91: 855–862, 2004.

878 D'Esposito M, Postle BR. The dependence of span and delayed-response performance on prefrontal
879 cortex. *Neuropsychologia* 37: 1303–1315, 1999.

880 Dudchenko PA. An overview of the tasks used to test working memory in rodents. *Neurosci Biobehav*
881 *Rev* 28: 699–709, 2004.

882 Everling S, Tinsley CJ, Gaffan D, Duncan J. Filtering of neural signals by focused attention in the
883 monkey prefrontal cortex. *Nat Neurosci* 5: 671–676, 2002.

884 Frith CD, Friston K, Liddle PF, Frackowiak RS. Willed action and the prefrontal cortex in man: a study
885 with PET. *Proc Biol Sci* 244: 241–246, 1991.

886 Funahashi S. Space representation in the prefrontal cortex. *Prog Neurobiol* 103: 131–155, 2013.

887 Funahashi S, Bruce CJ, Goldman-Rakic PS. Mnemonic coding of visual space in the monkey's
888 dorsolateral prefrontal cortex. *J Neurophysiol* 61: 331–349, 1989.

889 Funahashi S, Bruce CJ, Goldman-Rakic PS. Visuospatial coding in primate prefrontal neurons revealed
890 by oculomotor paradigms. *J Neurophysiol* 63: 814–831, 1990.

891 Funahashi S, Bruce CJ, Goldman-Rakic PS. Neuronal activity related to saccadic eye movements in the
892 monkey's dorsolateral prefrontal cortex. *J Neurophysiol* 65: 1464–1483, 1991.

893 Funahashi S, Bruce CJ, Goldman-Rakic PS. Dorsolateral prefrontal lesions and oculomotor
894 delayed-response performance: evidence for mnemonic "scotomas". *J Neurosci* 13: 1479–1497,
895 1993a.

896 Funahashi S, Chafee MV, Goldman-Rakic PS. Prefrontal neuronal activity in rhesus monkeys
897 performing a delayed anti-saccade task. *Nature* 365: 753–756, 1993b.

898 Fuster JM. *The Prefrontal Cortex.* San Diego: Academic Press, 2008, 4th edition.

899 Goldman-Rakic PS, Funahashi S, Bruce CJ. Neocortical memory circuits. *Cold Spring Harb Symp*
900 *Quant Biol* 55: 1025–1038, 1990.

901 Haynes JD, Sakai K, Rees G, Gilbert S, Frith C, Passingham RE. Reading hidden intentions in the
902 human brain. *Curr Biol* 17: 323–328, 2007.

903 Hesselmann G, Kell CA, Eger E, Kleinschmidt A. Spontaneous local variations in ongoing neural
904 activity bias perceptual decisions. *Proc Natl Acad Sci U S A* 105: 10984–10989, 2008.

905 Hyder F, Phelps EA, Wiggins CJ, Labar KS, Blamire AM, Shulman RG. "Willed action": a functional
906 MRI study of the human prefrontal cortex during a sensorimotor task. *Proc Natl Acad Sci U S A*
907 94: 6989–6994, 1997.

908 Judge SJ, Richmond BJ, Chu FC. Implantation of magnetic search coils for measurement of eye
909 position: an improved method. *Vision Res* 20: 535–538, 1980.

910 Kane MJ, Engle RW. Working-memory capacity and the control of attention: the contributions of goal
911 neglect, response competition, and task set to stroop interference. *J Exp Psychol Gen* 132: 47–70,
912 2003.

913 Kenet T, Bibitchkov D, Tsodyks M, Grinvald A, Arieli A. Spontaneously emerging cortical
914 representations of visual attributes. *Nature* 425: 954–956, 2003.

915 Lau HC, Rogers RD, Haggard P, Passingham RE. Attention to intention. *Science* 303: 1208–1210,
916 2004a.

917 Lau HC, Rogers RD, Ramnani N, Passingham RE. Willed action and attention to the selection of action.
918 *Neuroimage* 21: 1407–1415, 2004b.

919 Lebedev MA, Messinger A, Kralik JD, Wise SP. Representation of attended versus remembered
920 locations in prefrontal cortex. *PLoS Biol* 2: e365, 2004.

921 Lennert T, Martinez-Trujillo J. Strength of response suppression to distracter stimuli determines
922 attentional-filtering performance in primate prefrontal neurons. *Neuron* 70: 141–152, 2011.

923 Lennert T, Martinez-Trujillo JC. Prefrontal neurons of opposite spatial preference display distinct target
924 selection dynamics. *J Neurosci* 33: 9520–9529, 2013.

925 Martinez-Conde S, Macknik SL, Hubel DH. Microsaccadic eye movements and firing of single cells in
926 the striate cortex of macaque monkeys. *Nat Neurosci* 3: 251–258, 2000.

927 Matsushima A, Tanaka M. Different neuronal computations of spatial working memory for multiple
928 locations within versus across visual hemifields. *J Neurosci* 34: 5621–5626, 2014.

929 Messinger A, Lebedev MA, Kralik JD, Wise SP. Multitasking of attention and memory functions in the
930 primate prefrontal cortex. *J Neurosci* 29: 5640–5653, 2009.

931 Miller EK, Cohen JD. An integrative theory of prefrontal cortex function. *Annu Rev Neurosci* 24:
932 167–202, 2001.

933 Miyake A, Friedman NP, Emerson MJ, Witzki AH, Howerter A, Wager TD. The unity and diversity of
934 executive functions and their contributions to complex "frontal lobe" tasks: a latent variable
935 analysis. *Cogn Psychol* 41: 49–100, 2000.

936 Mochizuki K, Funahashi S. Opposing history effect of preceding decision and action in the free choice
937 of saccade direction. *J Neurophysiol* 112: 923–932, 2014.

938 Mottaghy FM, Gangitano M, Sparing R, Krause BJ, Pascual-Leone A. Segregation of areas related to
939 visual working memory in the prefrontal cortex revealed by rTMS. *Cereb Cortex* 12: 369–375,
940 2002.

941 Müller NG, Machado L, Knight RT. Contributions of subregions of the prefrontal cortex to working
942 memory: evidence from brain lesions in humans. *J Cogn Neurosci* 14: 673–686, 2002.

943 Ogawa T, Komatsu H. Differential temporal storage capacity in the baseline activity of neurons in
944 macaque frontal eye field and area V4. *J Neurophysiol* 103: 2433–2445, 2010.

945 Platt ML, Glimcher PW. Neural correlates of decision variables in parietal cortex. *Nature* 400: 233–238,
946 1999.

947 Procyk E, Goldman-Rakic PS. Modulation of dorsolateral prefrontal delay activity during self-organized
948 behavior. *J Neurosci* 26: 11313–11323, 2006.

949 R Core Team. *R: A Language and Environment for Statistical Computing*. R Foundation for Statistical
950 Computing, Vienna, Austria, 2015.

951 Rainer G, Asaad WF, Miller EK. Memory fields of neurons in the primate prefrontal cortex. *Proc Natl*
952 *Acad Sci U S A* 95: 15008–15013, 1998.

953 Rao SG, Williams GV, Goldman-Rakic PS. Isodirectional tuning of adjacent interneurons and
954 pyramidal cells during working memory: evidence for microcolumnar organization in PFC. *J*
955 *Neurophysiol* 81: 1903–1916, 1999.

956 Robinson DA. A method of measuring eye movement using a scleral search coil in a magnetic field.
957 *IEEE Trans Biomed Eng* 10: 137–145, 1963.

958 Rolls ET, Deco G. Prediction of decisions from noise in the brain before the evidence is provided. *Front*
959 *Neurosci* 5: 33, 2011.

960 Rowe JB, Toni I, Josephs O, Frackowiak RS, Passingham RE. The prefrontal cortex: response selection
961 or maintenance within working memory? *Science* 288: 1656–1660, 2000.

962 Sakai K, Rowe JB, Passingham RE. Active maintenance in prefrontal area 46 creates distractor-resistant
963 memory. *Nat Neurosci* 5: 479–484, 2002.

964 Saperstein AM, Fuller RL, Avila MT, Adami H, McMahon RP, Thaker GK, Gold JM. Spatial working
965 memory as a cognitive endophenotype of schizophrenia: assessing risk for pathophysiological
966 dysfunction. *Schizophr Bull* 32: 498–506, 2006.

967 Sawaguchi T, Iba M. Prefrontal cortical representation of visuospatial working memory in monkeys
968 examined by local inactivation with muscimol. *J Neurophysiol* 86: 2041–2053, 2001.

969 Shadlen MN, Newsome WT. Motion perception: seeing and deciding. *Proc Natl Acad Sci U S A* 93:
970 628–633, 1996.

971 Shadlen MN, Newsome WT. Neural basis of a perceptual decision in the parietal cortex (area LIP) of
972 the rhesus monkey. *J Neurophysiol* 86: 1916–1936, 2001.

973 Shenoy KV, Sahani M, Churchland MM. Cortical control of arm movements: a dynamical systems
974 perspective. *Annu Rev Neurosci* 36: 337–359, 2013.

975 Soon CS, Brass M, Heinze HJ, Haynes JD. Unconscious determinants of free decisions in the human
976 brain. *Nat Neurosci* 11: 543–545, 2008.

977 Tremblay S, Pieper F, Sachs A, Martinez-Trujillo J. Attentional filtering of visual information by
978 neuronal ensembles in the primate lateral prefrontal cortex. *Neuron* 85: 202–215, 2015.

979 Tsodyks M, Kenet T, Grinvald A, Arieli A. Linking spontaneous activity of single cortical neurons and
980 the underlying functional architecture. *Science* 286: 1943–1946, 1999.

981 Wang XJ. Decision making in recurrent neuronal circuits. *Neuron* 60: 215–234, 2008.

982 Wang XJ. The prefrontal cortex as a quintessential "cognitive-type" neural circuit: Working memory
983 and decision making. In: *Principles of Frontal Lobe Function.*, edited by Stuss DT, Knight RT,
984 Oxford, UK: Oxford University Press, 2013.

985 Wang XJ, Tegnér J, Constantinidis C, Goldman-Rakic PS. Division of labor among distinct subtypes of
986 inhibitory neurons in a cortical microcircuit of working memory. *Proc Natl Acad Sci U S A* 101:
987 1368–1373, 2004.

988 Watanabe K, Funahashi S. Prefrontal delay-period activity reflects the decision process of a saccade
989 direction during a free-choice ODR task. *Cereb Cortex* 17 Suppl 1: i88–100, 2007.

990 Watanabe K, Igaki S, Funahashi S. Contributions of prefrontal cue-, delay-, and response-period activity
991 to the decision process of saccade direction in a free-choice ODR task. *Neural Netw* 19:
992 1203–1222, 2006.

993 Zarahn E, Aguirre G, D'Esposito M. Replication and further studies of neural mechanisms of spatial
994 mnemonic processing in humans. *Brain Res Cogn Brain Res* 9: 1–17, 2000.

995 Zarahn E, Aguirre GK, D'Esposito M. Temporal isolation of the neural correlates of spatial mnemonic
996 processing with fMRI. *Brain Res Cogn Brain Res* 7: 255–268, 1999.

997

Figure Captions

Figure 1:

(**a**) Task configuration. Schematic illustration of the two tasks. In the ICT, the monkey was required to make a memory-guided saccade toward the cued location. In the FCT, the monkey needed to choose one of two cued locations before making a saccade. (**b**) Preference indices (bars) and response times (lines) of each monkey averaged across eight bins of absolute directions. Preference index was expected to be 0.25 if the monkey does not exhibit directional preference. (**c**) Choice proportions and response times in the FCT for rotated cue locations relative to the receptive field of the neurons. Proportion of T_{in} choice (left) was calculated for each of the T_{in} vs T_{ipsi}, T_{in} vs T_{contra}, and T_{in} vs T_{opp} pair condition, along with the total proportion calculated by collapsing the pair conditions. Response times (middle) and normalized response times (right) were averaged for each response direction, along with the grand average by collapsing all the directions.

Figure 2:

Activity of two representative neurons. Neuronal firing in each condition was plotted separately for the ICT (top row) and three pair conditions that included T_{in} as one of the two cues in the FCT (bottom three rows; T_{in} vs T_{ipsi}, T_{in} vs T_{contra}, and T_{in} vs T_{opp} conditions). The left half of each panel is aligned to the time from cue onset and the right half is aligned to saccade offset. Different colors in the histograms and rastergrams correspond to different directions of saccades. Both neurons exhibited directionally selective transient activation to presentation of the cue in the ICT. In each pair condition of the FCT, the left neuron (**a**) exhibited nearly equivalent activation to the presented cues regardless of which cue location was chosen later in that trial. In the right neuron (**b**), the strength of the transient response to the cues in the FCT was significantly larger when it was followed by the animal choosing the neuron's preferred direction, even though the T_{in} cue was presented along with the T_{out} cue in all three pair conditions.

Figure 3:

Population histograms and the change in ROC values in directionally selective cue-period neurons. (**a, c**) Averaged histograms and the ROC transition in the ICT. Fifty-nine neurons exhibited a significant directionally selective transient response to the cue in the ICT. Different colors indicate different directions of saccades. In the ICT, neuronal activity decreased with presentation of the cue at a location other than the

neuron's preferred direction (T_{in}), but the strength of the suppression was equivalent in the three T_{out} conditions. (**b, d**) Averaged histograms and the ROC transition in the FCT. In the FCT, the neurons exhibited differential activation that predicted the animal's subsequent choice of saccade direction. Different colors indicate the three pair conditions under investigation in the FCT. Solid and dotted lines in the histograms indicate the choice of the T_{in} and T_{out} directions later in that trial, respectively. The difference between solid and dotted lines with the same color (choice-predictive activity) was evident in the cue period, but actually started to appear before cue onset. An ROC analysis showed the same result. The increase in the ROC values from 0.5 started 750 ms before the start of the cue period.

Figure 4:

Population histograms of neurons with and without choice-predictive activity in the pre-cue and cue periods. Conventions for the histograms are the same as those in Fig. 2. Activity for T_{in} (solid) and T_{out} (dotted) choice trials in the three FCT pair conditions were plotted separately for choice-predictive (**a**, n = 38) and unpredictive (**b**, n = 21) neurons. Choice-predictive neurons also exhibited directionally selective activity during the delay period.

Figure 5:

Characteristics of firing properties of choice-predictive neurons. (**a**) Correlation between persistent directionally selective activity and choice-predictive activity. The strength of directionally selective activity in the delay period of the ICT (transverse axis, ROC values between T_{in} and T_{out} trials in 1000–1500 ms after the start of the delay period) was closely correlated with the strength of choice-predictive activity in the pre-cue and cue periods of the FCT (vertical axis, ROC values between T_{in} and T_{out} trials in -1000 to 500 ms from cue onset). (**b**) Comparison of baseline sustainability between choice-predictive (black) and choice-unpredictive (gray) neurons using different lengths of intervals. Choice-predictive neurons were characterized by a greater sustainability of activation even when the two bins were separated by a long interval. (**c–i**) Comparison of firing properties and animal's behavior between choice-predictive and unpredictive neurons. (**c**) Strength of persistent delay-period activity in the ICT. (**d**) Baseline sustainability for 400-ms interval. (**e**) Serial correlation of ISI. (**f**) Absolute direction of the receptive field (μ). Dots indicate the center of the receptive field and error bars indicate the size. Zero corresponds to horizontal direction contralateral to the recorded hemisphere, and positive and negative values indicate upper and lower direction from the horizontal meridian, respectively. (**g**) Size of the receptive field ($1/\sqrt{\beta}$). (**h**) Proportion of T_{in} choice in each pair condition and total proportion of T_{in} choice by collapsing pair

conditions. (**i**) Difference of response times between T_{in} choice and T_{out} choice trials. Choice-predictive neurons were characterized by their high persistence of activation (**c–e**) compared to choice-unpredictive neurons, without differences in absolute direction and size of the receptive fields (**f, g**) and the animal's behavior (**h, i**).

Figure 6:

Dynamics of neuronal activation using the state space based on a principal component analysis. (**a, b**) The activity of PFC neurons in each of the ICT (**a**) and FCT (**b**) conditions are shown as trajectories inside a 3-D principal component space. The activity around the cue and delay periods (from the start of the fixation period to 1500 ms after the start of the delay period) in both the ICT and FCT was collectively used to construct a state space. The letters in the panels show the start of the pre-cue (P), cue (C) and delay (D) periods, respectively. In the ICT (**a**), the activity of PFC neurons were indistinguishable at the start of the cue period. The trajectory in T_{in} cue condition then started to diverge from that in T_{out} cue conditions. In the FCT (**b**), the trajectories for T_{in} choice trials took similar courses to those for T_{in} cue condition in the ICT, while those for T_{out} choice trials resembled those for T_{out} cue conditions in the ICT. However, there was little separation between the trajectories for the T_{in} and T_{out} choice trials in the T_{in} vs T_{ipsi} pair condition compared to the other pair conditions. (**c**)

The distance between the trajectories for T_{in} choice and T_{out} choice trials in the state space. The trajectories for trials with different choices immediately diverged from each other in the cue period in the T_{in} vs T_{contra}/T_{opp} conditions, but not in the T_{in} vs T_{ipsi} condition.

Figure 7:

Construction of spatial representation in the FCT. (**a, b**) Each line shows the correlation coefficients between the neuronal activation pattern at each time bin in a given FCT condition and that of the pre-response period in a corresponding ICT condition in which the monkey made the same response. Data are separately plotted for T_{in} choice (**a**) and T_{out} choice (**b**) trials. Different colors indicate different pair conditions in the FCT. Thick solid lines show ranges of significant correlation in each task condition. Triangles at the top show the onset of significant correlation that lasted through the delay period. In the T_{in} vs T_{contra}/T_{opp} pair conditions, significant correlation began around the start of the cue period. In the T_{in} vs T_{ipsi} pair condition, significant correlation was observed at the end of the cue period in T_{in} choice trials and was not observed in T_{out} choice trials. (**c**) Result of a similar correlation analysis calculated between T_{out} choice trials in the FCT and T_{in} cue trials in the ICT. The neuronal activation pattern in FCT trials with T_{out} choice started to diverge from that

in ICT trials with a T_{in} cue before the start of the cue period in the T_{in} vs T_{contra}/T_{opp} conditions. However, a significant negative correlation was not observed until the delay period in the T_{in} vs T_{ipsi} pair condition.

Fig. 1

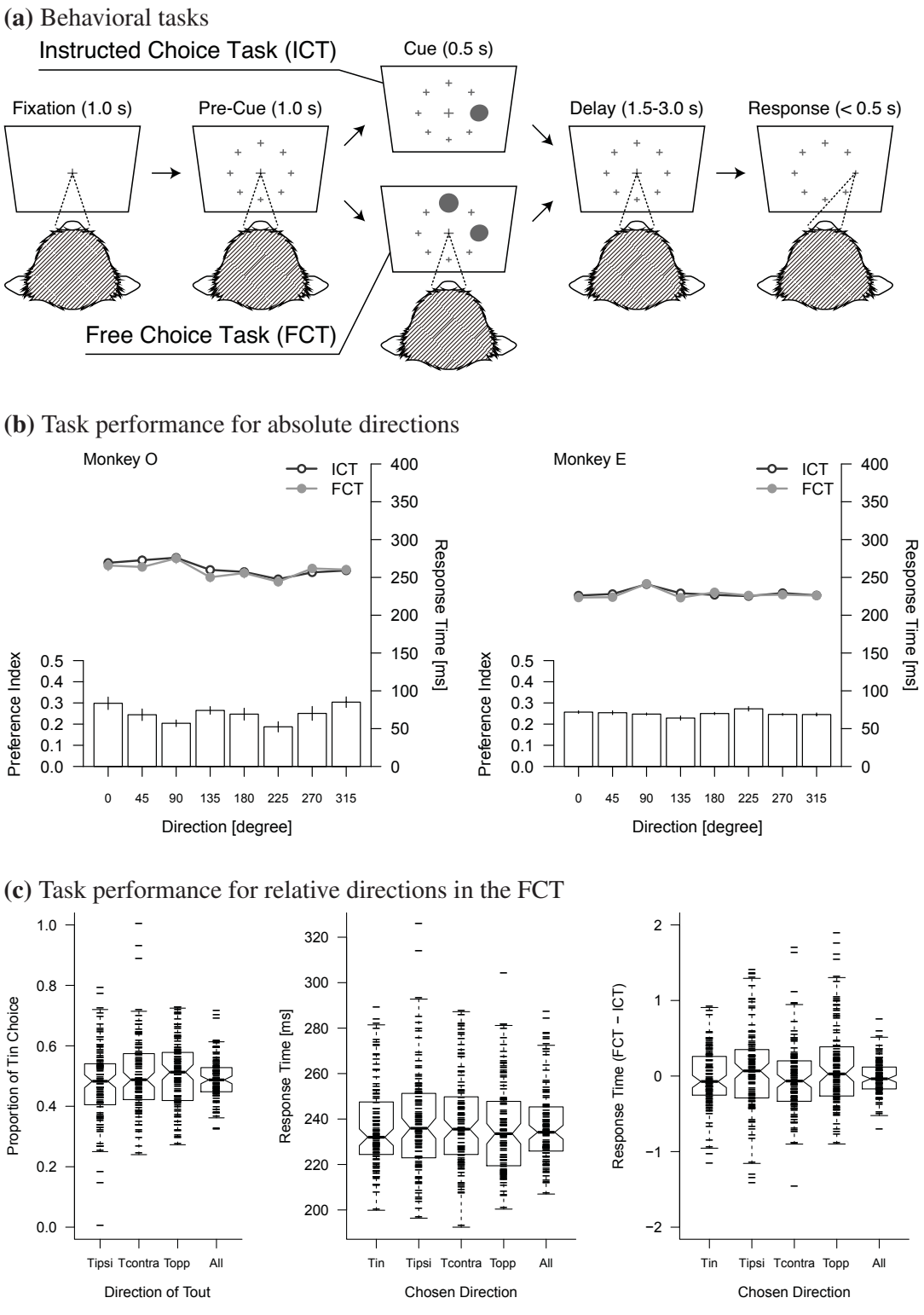
(a) Behavioral tasks
Instructed Choice Task (ICT)
Cue (0.5 s)
Fixation (1.0 s)
Pre-Cue (1.0 s)
Delay (1.5-3.0 s)
Response (< 0.5 s)
Free Choice Task (FCT)
(b) Task performance for absolute directions
Monkey O
Monkey E
ICT
FCT
Preference Index
Response Time [ms]
Direction [degree]
(c) Task performance for relative directions in the FCT
Proportion of Tin Choice
Response Time [ms]
Response Time (FCT − ICT)
Tipsi Tcontra Topp All
Tin Tipsi Tcontra Topp All
Direction of Tout
Chosen Direction

Fig. 2

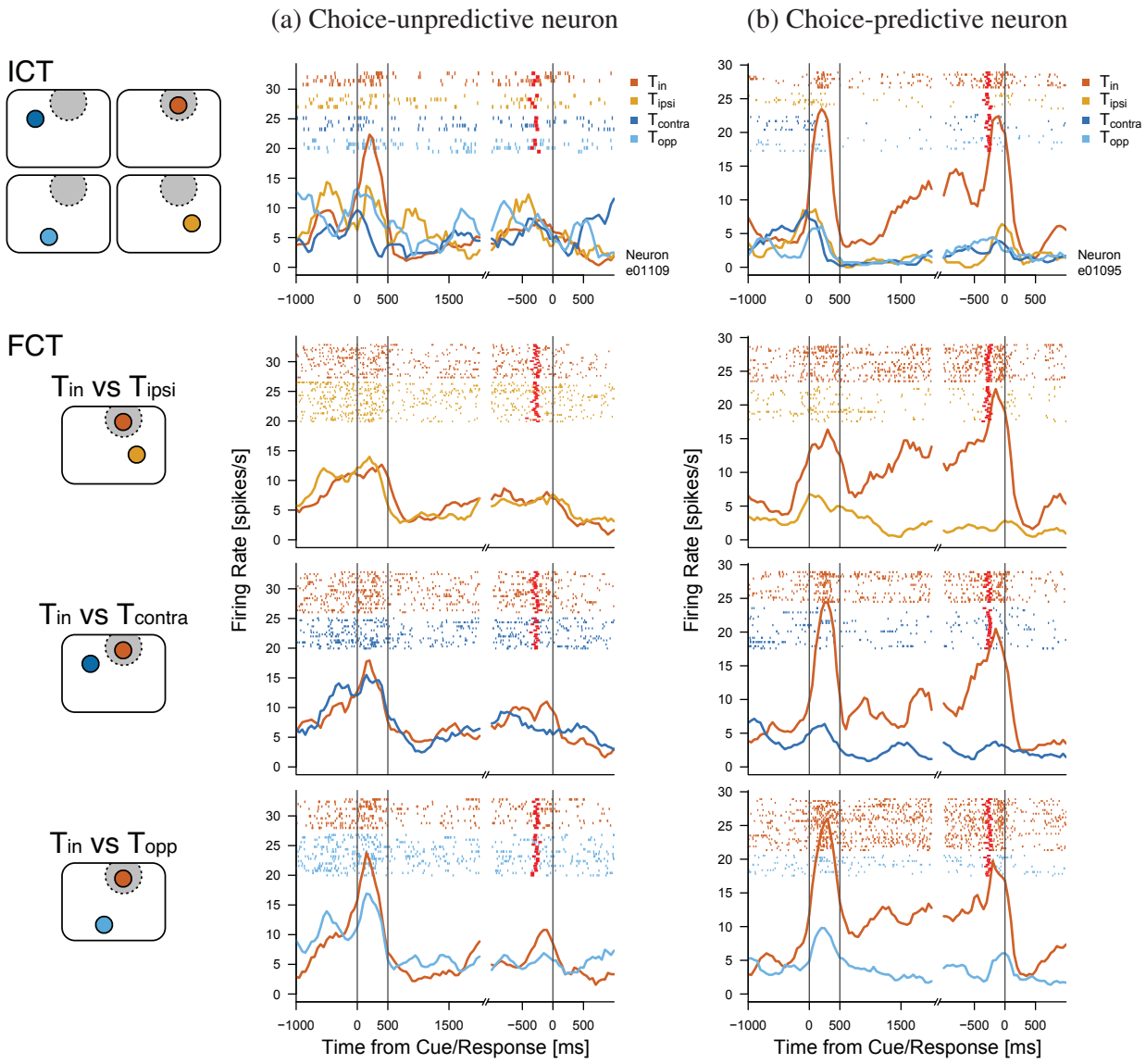
(a) Choice-unpredictive neuron
(b) Choice-predictive neuron
ICT
FCT
Tin vs Tipsi
Tin vs Tcontra
Tin vs Topp
Tin
Tipsi
Tcontra
Topp
Neuron e01109
Neuron e01095
Firing Rate [spikes/s]
Time from Cue/Response [ms]

Fig. 3

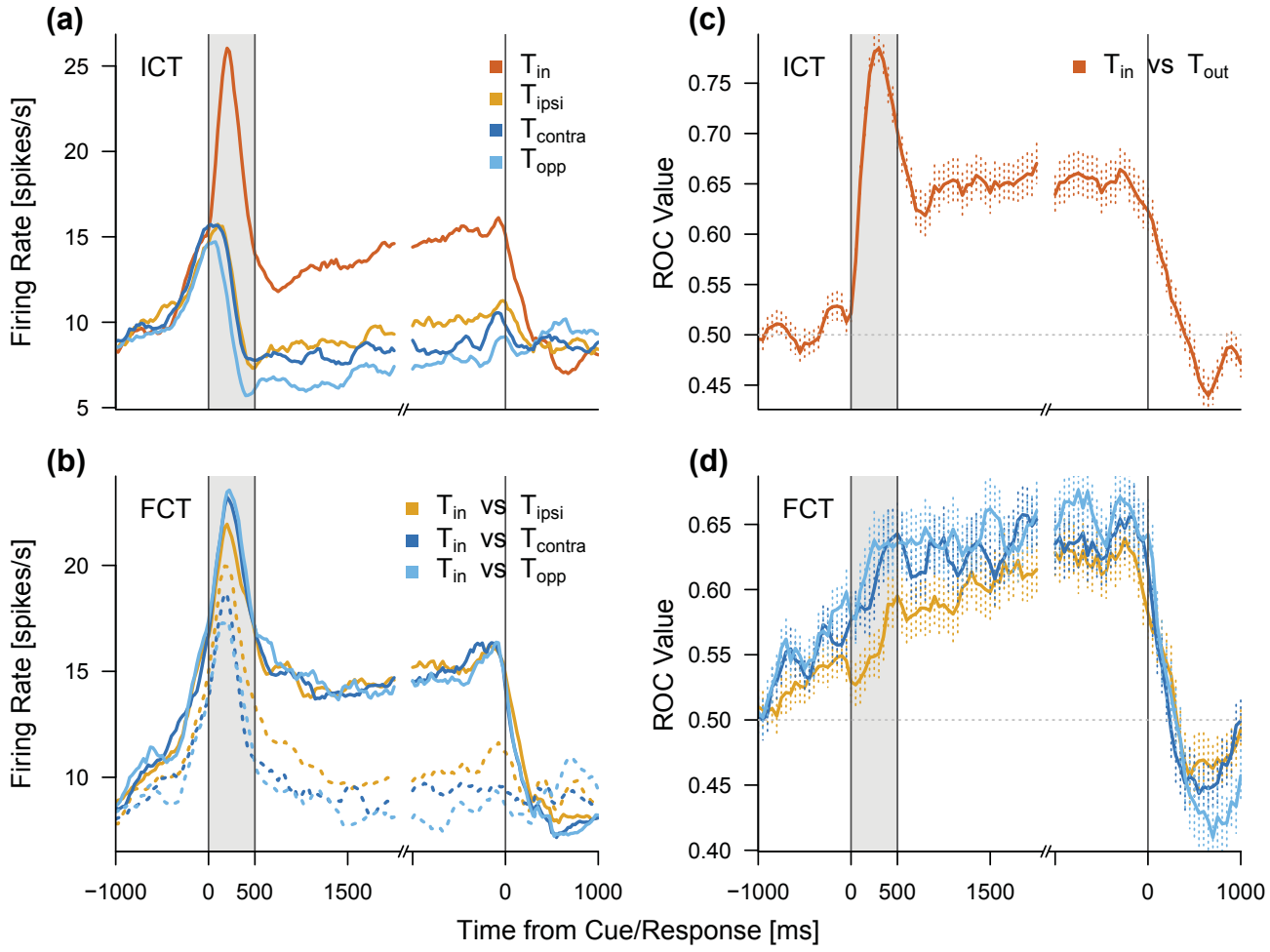
(a)
ICT
Firing Rate [spikes/s]
25
20
15
10
5
T_{in}
T_{ipsi}
T_{contra}
T_{opp}
(c)
ICT
ROC Value
0.75
0.70
0.65
0.60
0.55
0.50
0.45
T_{in} vs T_{out}
(b)
FCT
Firing Rate [spikes/s]
20
15
10
T_{in} vs T_{ipsi}
T_{in} vs T_{contra}
T_{in} vs T_{opp}
(d)
FCT
ROC Value
0.65
0.60
0.55
0.50
0.45
0.40
−1000
0
500
1500
0
1000
Time from Cue/Response [ms]

Fig. 4

(a) Choice-predictive neurons

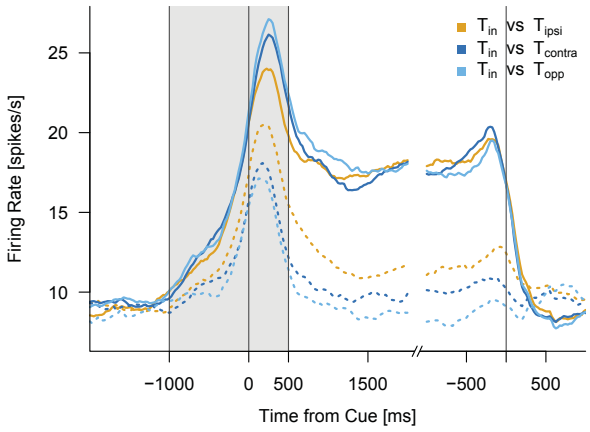

(b) Choice-unpredictive neurons

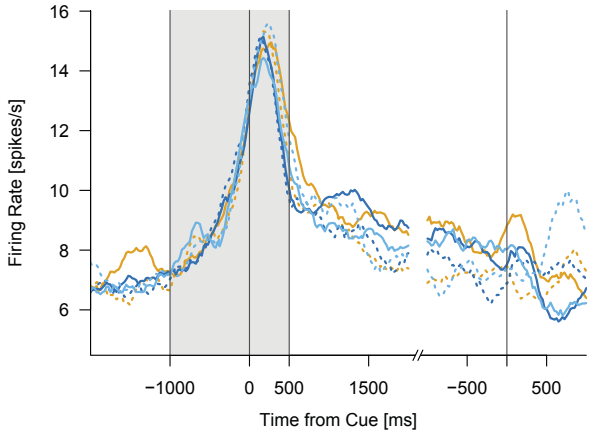

Fig. 5

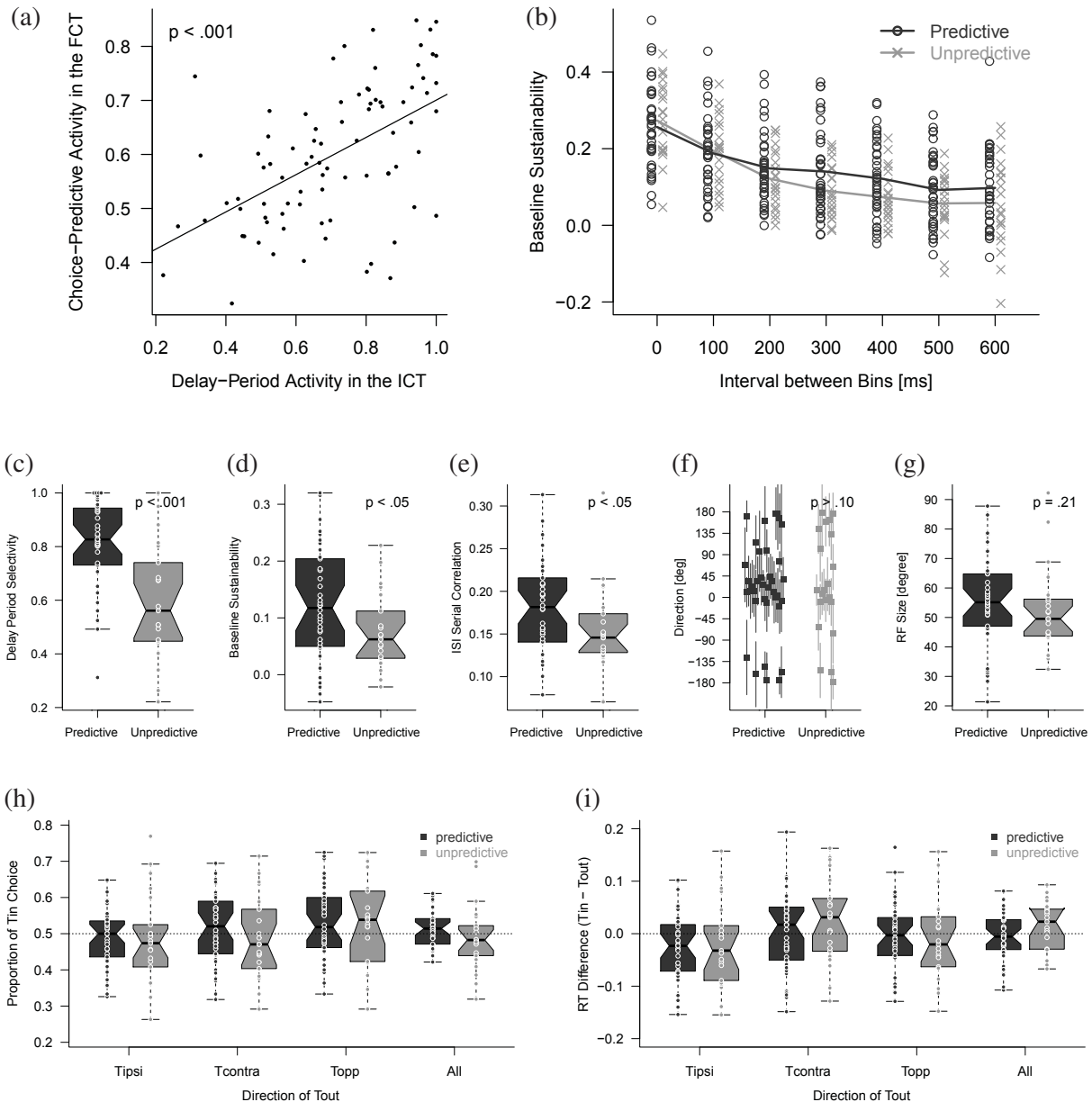
(a)
p < .001
Choice−Predictive Activity in the FCT
Delay−Period Activity in the ICT
(b)
Predictive
Unpredictive
Baseline Sustainability
Interval between Bins [ms]
(c)
p < .001
Delay Period Selectivity
(d)
p < .05
Baseline Sustainability
(e)
p < .05
ISI Serial Correlation
(f)
p > .10
Direction [deg]
(g)
p = .21
RF Size [degree]
(h)
predictive
unpredictive
Proportion of Tin Choice
Tipsi
Tcontra
Topp
All
Direction of Tout
(i)
predictive
unpredictive
RT Difference (Tin − Tout)
Tipsi
Tcontra
Topp
All
Direction of Tout

Fig. 6

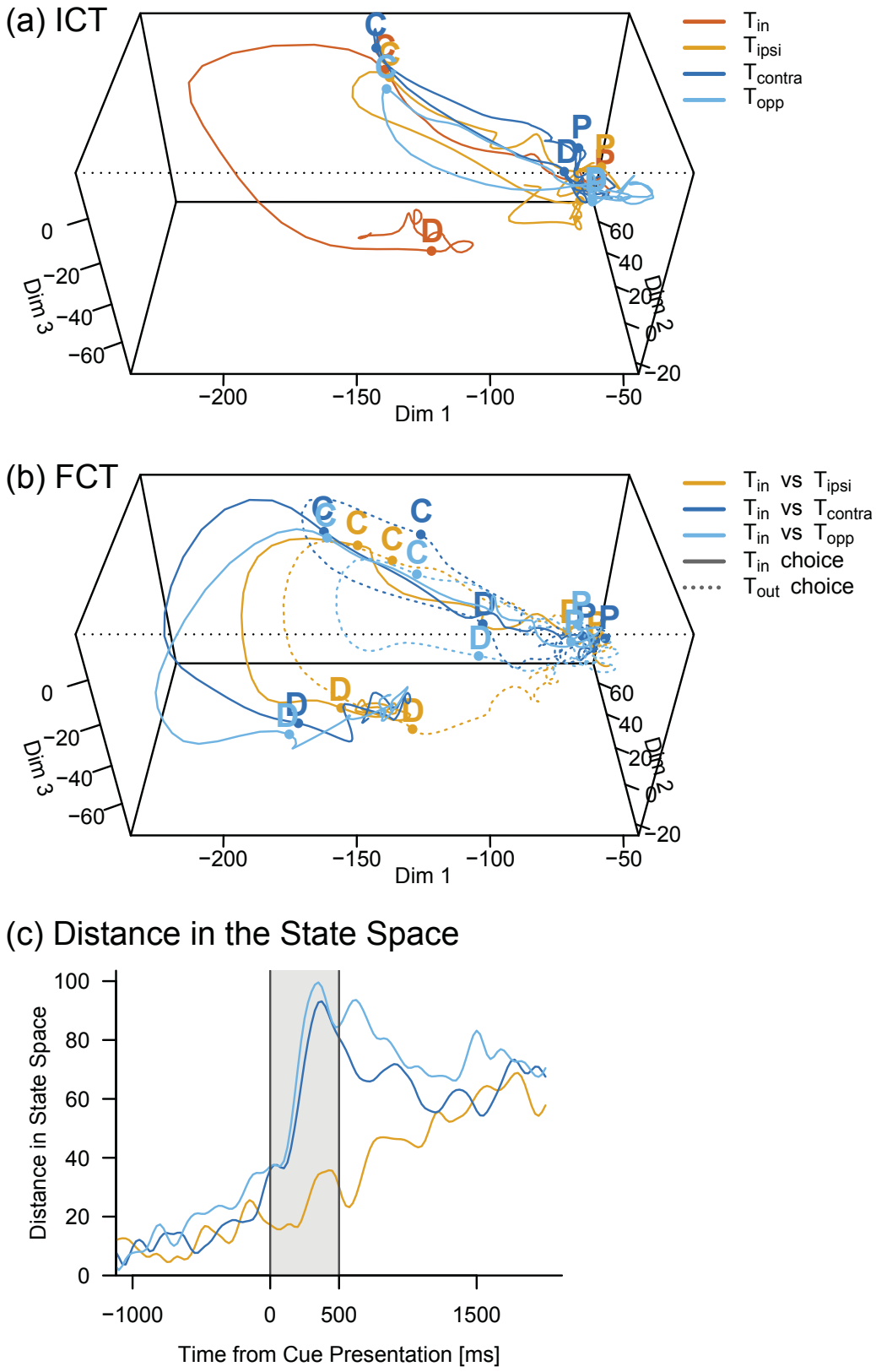
(a) ICT
T_{in}
T_{ipsi}
T_{contra}
T_{opp}
Dim 1
Dim 2
Dim 3
(b) FCT
T_{in} vs T_{ipsi}
T_{in} vs T_{contra}
T_{in} vs T_{opp}
T_{in} choice
T_{out} choice
(c) Distance in the State Space
Distance in State Space
Time from Cue Presentation [ms]

Fig. 7

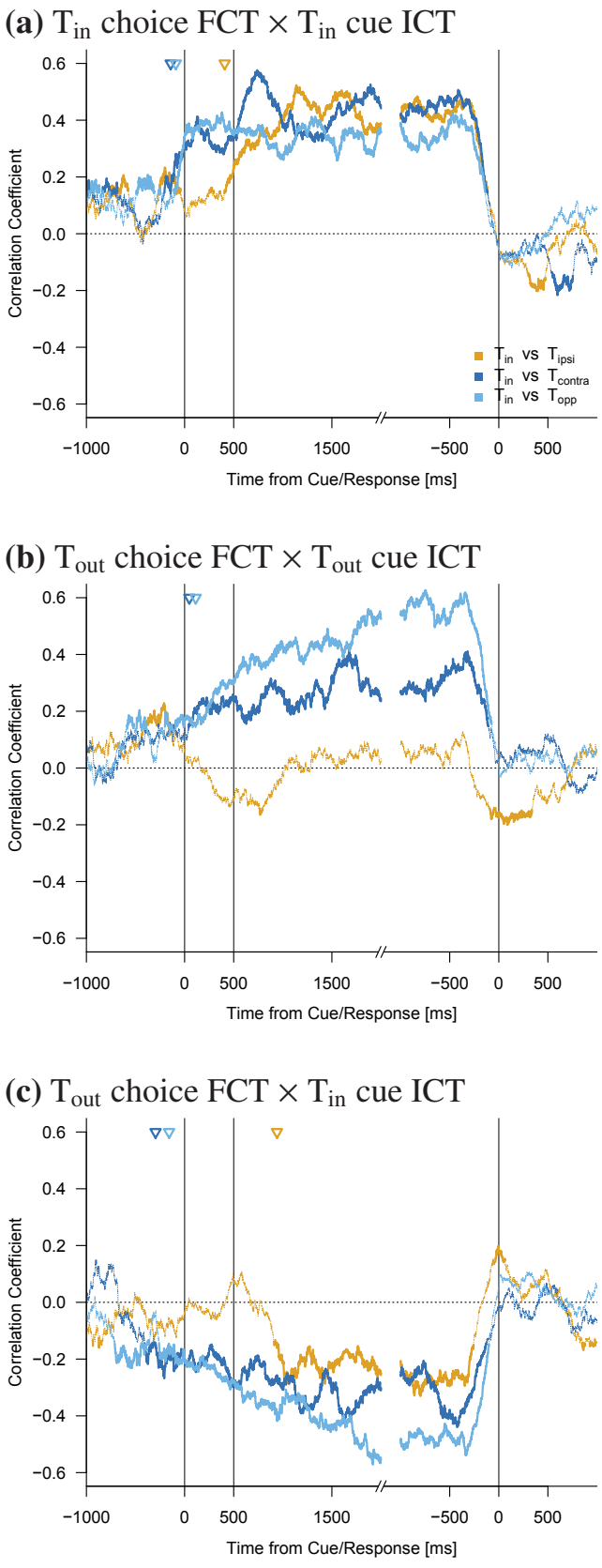
(a) T_{in} choice FCT × T_{in} cue ICT
Correlation Coefficient
0.6
0.4
0.2
0.0
−0.2
−0.4
−0.6
T_{in} vs T_{ipsi}
T_{in} vs T_{contra}
T_{in} vs T_{opp}
−1000
0
500
1500
−500
0
500
Time from Cue/Response [ms]
(b) T_{out} choice FCT × T_{out} cue ICT
Correlation Coefficient
Time from Cue/Response [ms]
(c) T_{out} choice FCT × T_{in} cue ICT
Correlation Coefficient
Time from Cue/Response [ms]